Letter | Editors' Suggestion

Stability of quasiperiodic superconductors

Nicole S. Ticea,[1] Julian May-Mann,[2] Jiewen Xiao,[3] Erez Berg,[3] and Trithep Devakul[2]
[1]*Department of Applied Physics, Stanford University, Stanford, California 94305, USA*
[2]*Department of Physics, Stanford University, Stanford, California 94305, USA*
[3]*Department of Condensed Matter Physics, Weizmann Institute of Science, Rehovot 76100, Israel*

(Received 9 May 2024; accepted 17 July 2024; published 1 August 2024)

We study the effects of quasiperiodicity on the stability of conventional and unconventional superconductors. Quasiperiodicity is modeled using the three-dimensional Aubry-André (AA) model, a system in which electrons are coupled to a translation-symmetry-breaking potential that is incommensurate with the underlying lattice. Upon increasing the strength of the quasiperiodic potential, the single-particle eigenstates undergo a transition from ballistic to diffusive character. We find that, in the ballistic regime, the system a weak-coupling instability towards both *s*-wave and *p*-wave superconductivity. In contrast, only the conventional *s*-wave instability survives in the diffusive regime. Our result suggest a version of Anderson's theorem for quasiperiodic systems, relating the normal state dynamics to the stability of conventional and unconventional superconductivity.

DOI: 10.1103/PhysRevB.110.L060501

Introduction. Quasiperiodic materials have been studied by crystallographers since the early 1980s [1], though evidence of a natural quasicrystal did not arise until 2009 with the discovery of icosahedrite [2]. Since then, interest in the field has surged with the realization of quasicrystals in a wide range of tunable systems, including optical [3–9] and photonic lattices [10–14], cavity polaron devices [15], and moiré materials [16,17]. With tunability comes the opportunity to study how quasiperiodicity not only disrupts or stabilizes known physics, but can also engender new phenomena [18–35].

In this paper, we seek to understand how quasiperiodicity affects conventional (*s*-wave) and unconventional (non-*s*-wave) superconductivity. We are motivated, in part, by the existence of superconductivity in moiré systems [17,36–39]. Although all twisted moiré graphene systems exhibit a quasiperiodic arrangement of atoms at generic twist angles [40], the low-energy electronic behavior in most paradigmatic structures (e.g., twisted bilayer graphene) is determined by an emergent long-wavelength moiré periodicity [41]. Recent studies, however, suggest that it is possible to realize superconductivity in an incommensurate trilayer system, in which even the low energy physics is quasiperiodic [42,43]. This discovery has the potential to yield new insight into the nature of superconductivity in moiré graphene. Because translational symmetry is broken in systems with either quasiperiodicity or random disorder, one might expect quasiperiodic systems to behave similarly to those with disorder. Quasiperiodic lattices, however, possess multiple periodic orders that are incommensurate with each other [44]. Because of these periodic orders, quasiperiodic systems are highly structured in momentum space; the diffraction pattern of the ideal, infinite quasicrystal can be characterized by a self-similar arrangement of Bragg peaks, densely tiled throughout reciprocal space [45]. This results in dynamical properties that are qualitatively distinct from the randomly-disordered case [46]. A paradigmatic quasiperiodic system is the Aubry-André (AA) model in one spatial dimension (1D), a model of fermions on a lattice subject to a periodically modulating onsite potential that is incommensurate with the lattice. As the potential strength is tuned, this system undergoes a transition at finite potential strength from a phase with ballistic states (i.e., momentum-space localized states) to a phase with real-space localized states. The AA model can also be generalized to 3D [47], where it displays two finite-potential-strength transitions: first from a ballistic to a diffusive phase, and then from the diffusive phase to a real-space-localized phase. In contrast, in random systems in 3D, the ballistic-to-diffusive transition occurs at infinitesimal disorder strength.

A number of works have considered superconductivity in other quasiperiodic systems, such as the Penrose lattice [48–55] and the 1D AA model [56], where an enhancement of *s*-wave superconductivity is observed near the ballistic-to-localized transition [57] An advantage of working with the AA model is that the quasiperiodicity can be tuned by adjusting the strength of the potential, in the same way that one can study the effects of random disorder simply by tuning the strength of the disordered potential. In randomly disordered systems, low levels of non-magnetic disorder do not affect *s*-wave superconductivity; this is Anderson's theorem for disordered superconductors [58]. Unconventional superconductors (i.e., those with higher angular momentum pairing symmetry), however, are fragile to even small amounts of random disorder in three dimensions [59,60]. This motivates us to ask if quasiperiodicity affects conventional and unconventional superconductivity in the same manner as does random disorder, a previously unaddressed question in the literature.

In the 3D AA model, we find that weak-coupling instabilities of both conventional and unconventional superconductors are robust to small, but finite, quasiperiodicity. For unconventional superconductivity, the instability vanishes once the strength of the quasiperiodic potential exceeds a critical value coinciding with the transition from ballistic to diffusive transport. For conventional superconductivity, the weak coupling instability persists throughout the ballistic and diffusive

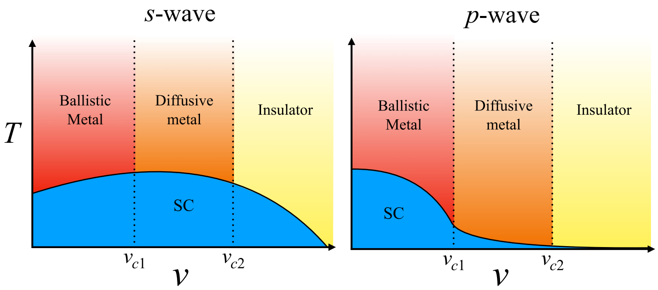

FIG. 1. Schematic phase diagram for *s*- and *p*-wave superconductivity in the 3D Aubry-André model as a function of quasiperiodic potential strength. In the normal state, ballistic-to-diffusive and diffusive-to-localized transitions occur at $v = v_{c1}$ and $v = v_{c2}$ respectively.

phases. We find that the T_c for unconventional superconductivity is strongly suppressed in the diffusive and localized regimes, while the T_c for conventional superconductivity only starts to become suppressed in the localized phase. These findings are illustrated in Fig. 1. For both conventional and unconventional superconductivity, we find that the suppression of T_c is primarily due to phase fluctuations. Taken together, these results suggest a generalization of Anderson's theorem of disordered superconductors to quasiperiodic systems.

Model. Our starting point is the 3D generalization of the AA model [47]:

$$H = \sum_{\sigma}\sum_{\boldsymbol{r}}\sum_{i=1}^{3}\left(e^{i\phi_i}c^{\dagger}_{\boldsymbol{r}+\hat{u}_i\sigma}c_{\boldsymbol{r}\sigma} + \text{H.c.}\right) + H_{\text{QP}}. \quad (1)$$

The sum is over all sites $\boldsymbol{r}$ on an $L\times L\times L$ cubic lattice, $\{\phi_i\}$ are arbitrary phases that twist the periodic boundary conditions in all three directions, $\{\hat{u}_i\}$ are the lattice basic vectors, and $c_{\boldsymbol{r}\sigma}$ annihilates a fermion on site $\boldsymbol{r}$ with spin $\sigma = \uparrow, \downarrow$. The quasiperiodic potential is specified by

$$H_{\text{QP}} = 2v\sum_{\boldsymbol{r}}\sum_{i=1}^{3}\cos\left(2\pi\sum_{j=1}^{3}B_{ij}r_j + \phi_i\right)n_{\boldsymbol{r}}, \quad (2)$$

where $n_{\boldsymbol{r}} = \sum_\sigma c^{\dagger}_{\boldsymbol{r}\sigma}c_{\boldsymbol{r}\sigma}$, and v controls the strength of the quasiperiodic potential. The phases $\{\phi_i\}$ amount to an overall arbitrary shift of the cosine potential, and are taken to be the same as in Eq. (1) so that this model is self-dual upon transforming from real to momentum space and sending $v \to 1/v$ [47,61].

The matrix $\mathbf{B}$ determines the characteristics of this model most relevant to this paper. If we wish to define a quasiperiodic system, then we impose that $\sum_j B_{ij}r_j \notin \mathbb{Z}^3$ for all $\boldsymbol{r} \neq 0$. Here we take $\mathbf{B} = Q\mathbf{R}(\theta)$, where $Q = \frac{\sqrt{5}-1}{2}$ is the golden ratio and $\mathbf{R}(\theta)$ can be thought of as a reflection about the line $y = z$ followed by three Euler rotations $(Y_\theta X_\theta Z_\theta)$ around an angle θ, which we take here to be $\pi/7$ [62]. In practice, it is useful to define the AA model on a finite-size system on periodic boundary conditions. To do so, we must enforce periodicity in system size L, which amounts to picking a rational approximant for $\mathbf{B}$ such that $L\mathbf{B}$ is an integer-valued matrix. We also require the approximate form of $\mathbf{B}$ to satisfy $\gcd(\det(L\mathbf{B}), L) = 1$; as a result, the only translation symmetry preserved by the cosine potential is $\boldsymbol{r} \to \boldsymbol{r} + L\boldsymbol{n}$, with $\boldsymbol{n} \in \mathbb{Z}^3$. On top of breaking translation symmetry, the quasiperiodic potential also breaks rotation symmetry around any axis. The model, however, remains invariant under inversion, $\boldsymbol{r} \to -\boldsymbol{r}$ when the phases $\{\phi_i\}$ are equal to 0 or π.

This model is self-dual at $v_{\text{SD}} = 1$. Previous studies on this model [47] report an extended diffusive phase, bracketed on either side by a finite ballistic phase ($v < v_{c_1}$) and a real-space localized phase ($v > v_{c_2}$). The mean-square displacement of an initially localized particle scales $\propto t^2$ in the ballistic phase, $\propto t$ in the diffusive phase, and $\propto$ const. in the localized phase, where t is time [47]. We can also characterize these phases according to their inverse participation ratios (IPRs), which we define in real space as $\text{IPR}_{\boldsymbol{r}} = \sum_{\boldsymbol{r}}|\psi(\boldsymbol{r})|^4$, and in momentum space as $\text{IPR}_{\boldsymbol{k}} = \sum_{\boldsymbol{k}}|\psi(\boldsymbol{k})|^4$, where $\psi(\boldsymbol{r})$ and $\psi(\boldsymbol{k})$ are energy eigenstates of H in the position and momentum space bases respectively. In the localized phase, $\text{IPR}_{\boldsymbol{r}} \to 1$ and $\text{IPR}_{\boldsymbol{k}} \to 0$ in the $L \to \infty$ limit, while in the ballistic phase $\text{IPR}_{\boldsymbol{r}} \to 0$ and $\text{IPR}_{\boldsymbol{k}} \to 1$. In the diffusive phase, $\text{IPR}_{\boldsymbol{r}} \to 0$ and $\text{IPR}_{\boldsymbol{k}} \to 0$. We plot the IPRs for Eq. (1) as a function of v in Fig. 2. We estimate the value of v_{c1}, the critical point between the ballistic and diffusive phases, to be $\approx$0.5 for the states near half filling, as indicated by the dashed vertical line. We also calculate the IPRs for a corresponding 3D system with random disorder. Here, the random disorder potential is realized by making the phases ϕ_i fluctuate randomly with position: $\phi_i \to \phi_i(\boldsymbol{r})$, with $\phi_i \in [0, 2\pi]$ chosen randomly on each site. For random disorder, the system is in the diffusive phase for any small $v > 0$.

Cooper logarithm in quasiperiodic systems. BCS theory indicates that, in a clean system, the pairing susceptibility in the spin-singlet channel diverges as $\log(T)$ at low temperatures. We define the spin-singlet susceptibility in real space as

$$\chi^{s}_{\boldsymbol{r}\boldsymbol{r}';\boldsymbol{r}''\boldsymbol{r}'''} = \int_0^\beta d\tau[\langle c_{\boldsymbol{r}\downarrow}(\tau)c^{\dagger}_{\boldsymbol{r}''\downarrow}(0)\rangle\langle c_{\boldsymbol{r}'\uparrow}(\tau)c^{\dagger}_{\boldsymbol{r}'''\uparrow}(0)\rangle + \langle c_{\boldsymbol{r}\uparrow}(\tau)c^{\dagger}_{\boldsymbol{r}'''\uparrow}(0)\rangle\langle c_{\boldsymbol{r}'\downarrow}(\tau)c^{\dagger}_{\boldsymbol{r}''\downarrow}(0)\rangle], \quad (3)$$

where $c_{\boldsymbol{r}\sigma}(\tau)$ is the electron creation operator at imaginary time τ, and $\beta = 1/T$. If we treat χ^s as a $L^6\times L^6$ matrix, then its largest eigenvalue will scale $\propto \log(T)$ at low temperatures. This is the celebrated Cooper logarithm. For a system with interactions of the form $H_{\text{int}} = \sum_{\boldsymbol{r},\boldsymbol{r}'} V_{\boldsymbol{r}\boldsymbol{r}'}n_{\boldsymbol{r}}n_{\boldsymbol{r}'}$, the real-space linearized gap equation (LGE) can be expressed in terms of the pairing susceptibility in the spin-singlet channel as

$$\Delta^{s}_{\boldsymbol{r}\boldsymbol{r}'} = -\sum_{\boldsymbol{r}'',\boldsymbol{r}'''} V_{\boldsymbol{r},\boldsymbol{r}'}\chi^{s}_{\boldsymbol{r}\boldsymbol{r}';\boldsymbol{r}''\boldsymbol{r}'''}\Delta^{s}_{\boldsymbol{r}''\boldsymbol{r}'''}. \quad (4)$$

Here, $\Delta^s_{\boldsymbol{r}\boldsymbol{r}'}$ is the gap function for a pair of particles at $\boldsymbol{r}$ and $\boldsymbol{r}'$. The $\log(T)$ divergence of χ^s therefore guarantees a finite-temperature solution to the LGE for arbitrarily weak attractive interactions.

In the presence of random nonmagnetic impurities, *s*-wave superconductors will continue to exhibit this weak-coupling divergence well into the diffusive phase [58,63]. We contrast this behavior with that of spin-triplet (*p*-wave) superconductors. The pairing susceptibility for the $S_z = 0$ total spin

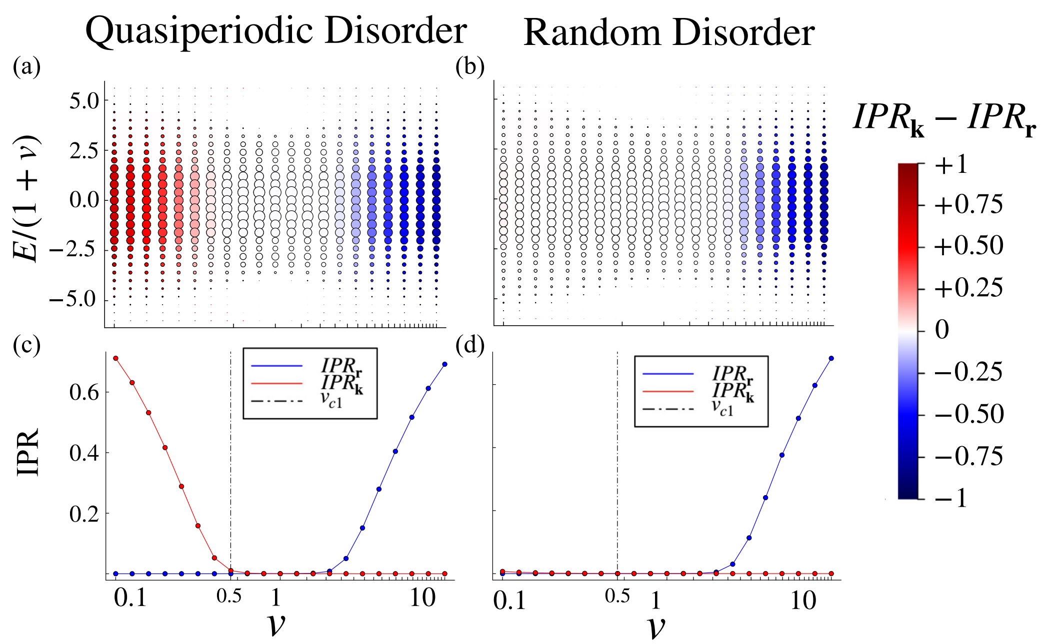

FIG. 2. Top row: At low v, the state is initially localized in momentum space (red); as v is increases, the state becomes real-space localized (blue). The size of the data points corresponds to the density of states. Bottom row: the IPRs as a function v along the $E/(1+v) = 0.75$ line cut.

configuration is

$$\chi^{\mathrm{p}}_{\boldsymbol{r}\boldsymbol{r}';\boldsymbol{r}''\boldsymbol{r}'''} = \int_0^\beta d\tau [\langle c_{\boldsymbol{r}\downarrow}(\tau)c^\dagger_{\boldsymbol{r}''\downarrow}(0)\rangle\langle c_{\boldsymbol{r}'\uparrow}(\tau)c^\dagger_{\boldsymbol{r}'''\uparrow}(0)\rangle - \langle c_{\boldsymbol{r}\uparrow}(\tau)c^\dagger_{\boldsymbol{r}'''\uparrow}(0)\rangle\langle c_{\boldsymbol{r}'\downarrow}(\tau)c^\dagger_{\boldsymbol{r}''\downarrow}(0)\rangle]. \tag{5}$$

In the case of random disorder, this susceptibility will not diverge for any finite amount of random disorder [59].

We aim to understand how the s-wave and p-wave susceptibilities behave in the 3D AA model. To this end, consider the uniform static pairing susceptibility,

$$\chi^{\mathrm{s/p},0}_{\boldsymbol{\delta},\boldsymbol{\delta}'} = \frac{1}{L^6}\sum_{\boldsymbol{r},\boldsymbol{r}'}\chi^{\mathrm{s/p}}_{\boldsymbol{r},\boldsymbol{r}+\boldsymbol{\delta};\boldsymbol{r}',\boldsymbol{r}'+\boldsymbol{\delta}'}. \tag{6}$$

Although we do not expect the solution to be spatially uniform for moderate-to-large strengths of the quasiperiodic disorder, $\chi^{\mathrm{s/p},0}_{\boldsymbol{\delta},\boldsymbol{\delta}'}$ will nevertheless capture any divergences present in the actual susceptibility so long as the two quantities possess finite overlap. The spatial average also neutralizes spurious contributions from rare superconducting regions [64], as the overlap of the uniform solution with any localized solutions goes to zero as L grows large.

Assuming pairing of time-reversed states, we calculate the uniform susceptibility [65] for the s-wave ($\chi^{\mathrm{s}0}_{0,0}$) and p_z-wave ($\chi^{\mathrm{p}0}_{\hat{z},\hat{z}}$) channels using Eq. (1) with a chemical potential of $\mu = 0.75(1+v)$ [66]. Results are shown in Fig. 3. For the randomly disordered potential, we average over different random configurations. For the quasiperiodic potential, we average over different phases $\{\phi_i\}$. It is worth noting that the averaged system possesses inversion symmetry in both cases.

We plot $-d\chi^{\mathrm{s/p},0}_{\delta\delta'}/d\log T$, the derivative of the uniform susceptibility with respect to the temperature. If this quantity goes to zero, the susceptibility saturates, and superconductivity exists only in the presence of finite strength interactions. Conversely, a plateau where $-d\chi^{\mathrm{s/p},0}_{\delta\delta'}/d\log T \neq 0$ is indicative of a $\log(T)$ divergence of the susceptibility at low temperatures, and, by extension, a weak-coupling superconducting instability. We find that the logarithmic divergence of the s-wave channel susceptibility is stable to both quasiperiodic and random potentials. In the p_z-wave channel, we find that the uniform susceptibility has a logarithmic divergence for $v < v_{c1} \approx 0.5$. Hence, there is a weak coupling instability in the p_z-wave channel throughout the ballistic phase of the model. However, in the diffusive and localized phases ($v > v_{c1}$) this logarithmic divergence is completely suppressed. We emphasize that the $\log(T)$ divergence of the susceptibility in both conventional and unconventional channels is stable for small but finite quasiperiodicity. This is unlike the case for random disorder, where a finite amount of disorder suppresses the logarithmic divergence in the p_z-wave channel.

Transition temperature. Having established the qualitative effects of quasiperiodic disorder on weakly-coupled superconductors, we now consider introducing finite-strength interactions to the 3D AA model,

$$H_{\mathrm{int}} = V_0\sum_{\boldsymbol{r}} n_{\boldsymbol{r}}n_{\boldsymbol{r}} + \frac{V_1}{2}\sum_{\langle \boldsymbol{r},\boldsymbol{r}'\rangle} n_{\boldsymbol{r}}n_{\boldsymbol{r}'}, \tag{7}$$

where $\langle\cdots\rangle$ indicates nearest neighbors. For the s-wave channel, we set $V_0 < 0$ and $V_1 = 0$, and for p-wave, we set $V_0 = 0$ and $V_1 < 0$. We treat the problem at a mean field level by using the following trial Hamiltonians and self-consistency equations:

$$H^{\mathrm{s}}_{\mathrm{MF}} = \frac{1}{2}\sum_{\boldsymbol{r}}[\Delta^{\mathrm{s}}_{\boldsymbol{r}\boldsymbol{r}}(c^\dagger_{\boldsymbol{r}\uparrow}c^\dagger_{\boldsymbol{r}\downarrow} - c^\dagger_{\boldsymbol{r}\downarrow}c^\dagger_{\boldsymbol{r}\uparrow}) + \mathrm{H.c.}], \tag{8}$$

$$\Delta^{\mathrm{s}}_{\boldsymbol{r},\boldsymbol{r}} = \frac{V_0}{2}[\langle c_{\boldsymbol{r},\downarrow}c_{\boldsymbol{r},\uparrow}\rangle - \langle c_{\boldsymbol{r},\uparrow}c_{\boldsymbol{r},\downarrow}\rangle], \tag{9}$$

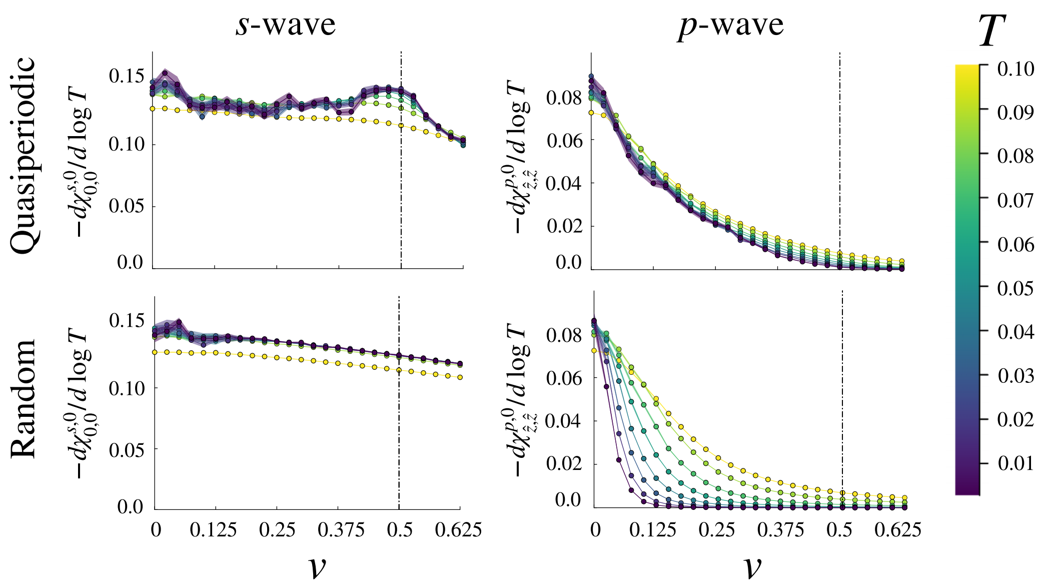

FIG. 3. Uniform susceptibilities for quasiperiodic (left) and random (disorder) potentials on a $23 \times 23 \times 23$ lattice with $\theta = \pi/7$ and $Q = (\sqrt{2} - 1)/2$ along the constant line cut $0.75 = \mu/(1 + \upsilon)$. The vertical dashed line indicates the ballistic-to-diffusive transition at $\upsilon = \upsilon_{c1}$. Error ribbons represent the standard error of the mean, which comes from averaging over $N \approx 35$ disorder realizations.

and

$$H_{\mathrm{MF}}^{\mathrm{p}} = \frac{1}{2} \sum_{\langle \boldsymbol{r}, \boldsymbol{r}' \rangle} \left[\Delta_{\boldsymbol{r}\boldsymbol{r}'}^{\mathrm{p}} \left(c_{\boldsymbol{r}\uparrow}^{\dagger} c_{\boldsymbol{r}'\downarrow}^{\dagger} + c_{\boldsymbol{r}\downarrow}^{\dagger} c_{\boldsymbol{r}'\uparrow}^{\dagger} \right) + \mathrm{H.c.} \right], \tag{10}$$

$$\Delta_{\boldsymbol{r},\boldsymbol{r}'}^{\mathrm{p}} = \frac{V_1}{2} [\langle c_{\boldsymbol{r}',\downarrow} c_{\boldsymbol{r},\uparrow} \rangle + \langle c_{\boldsymbol{r}',\uparrow} c_{\boldsymbol{r},\downarrow} \rangle], \tag{11}$$

for s- and p-wave respectively.

The mean-field transition temperature can be identified by studying solutions of the linearized gap equation. Given an interaction matrix $V_{\boldsymbol{r}\boldsymbol{r}'}$ defined as in Eq. (7), we estimate T_c^{LGE} by diagonalizing

$$M_{\boldsymbol{r}\boldsymbol{r}';\boldsymbol{r}''\boldsymbol{r}'''}^{\mathrm{s/p}} \equiv - \sum_{\boldsymbol{r}'',\boldsymbol{r}'''} V_{\boldsymbol{r}\boldsymbol{r}'} \chi_{\boldsymbol{r}\boldsymbol{r}';\boldsymbol{r}''\boldsymbol{r}'''}^{\mathrm{s/p}} \tag{12}$$

and determining the temperature at which the largest eigenvalue of $M^{\mathrm{s/p}}$ is equal to 1 [67].

The LGE solution is plotted using green markers in Fig. 4. For both s- and p-wave, we observe an initial decrease followed by an increase in T_c^{LGE} with υ. This latter increase in T_c^{LGE} is unphysical, in the sense that it does not correspond

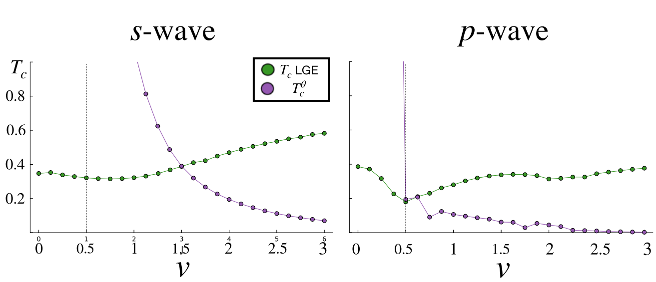

FIG. 4. T_c calculated for s-wave ($V_0 = -3, V_1 = 0$) and p-wave ($V_0 = 0, V_1 = -3$) superconductivity for a $11 \times 11 \times 11$ lattice. Green markers correspond to T_c^{LGE}, the transition temperature calculated from the linearized gap equation. Purple markers correspond to T_c^{θ}, the transition temperature as estimated from the superfluid stiffness.

to the transition into a state with zero resistance [64]. To understand why the LGE solution behaves in this way, it is important to keep in mind that T_c^{LGE} estimates the temperature at which a superconducting condensate first forms. However, this condensate may be localized to multiple small, nonoverlapping regions. In this setting, one should really think of the system as being composed of superconducting islands coupled to each other via weak Josephson-type coupling [68]. The resistance of such a state will only drop to zero when the different islands become phase coherent. If the coupling between different islands is weak, the phases might not cohere until the temperature is lowered *below* T_c^{LGE}.

To estimate the temperature at which phase coherence sets in, we assume that the only relevant degrees of freedom are the superconducting phases, and model the superconductor as an XY model. The temperature where phase coherence sets in is estimated as $T_c^{\theta} = \frac{A n_s(0)}{4m^*} a_{\mathrm{SC}}$ [68], where $n_s(0)$ is the geometric mean of the super fluid density at zero temperature [69,70], m^* is the effective mass of the electrons, $a_{\mathrm{SC}} = \min\{\sqrt{\pi}\xi_{\mathrm{SC}}, a_{\mathrm{L}}\}$; a_{L} is the lattice constant; ξ is the superconducting coherence length, $\xi = \upsilon_F/(\pi\Delta)$ [71]; and υ_F is the Fermi velocity calculated in the clean system. A is a dimensionless number of order unity that depends on the details of the short-distance physics, which we take to be 2.2 after Ref. [68]. The superfluid stiffness n_s and coherence length ξ are calculated by solving the BdG equations [Eqs. (9) and (11)].

Numerical results are shown in Fig 4. The true T_c of the system is $T_c = \min(T_c^{\mathrm{LGE}}, T_c^{\theta})$. For s-wave, T_c remains finite even into the localized phase $\upsilon > \upsilon_{c2}$. Conversely, T_c falls off sharply close to υ_{c1} for the p-wave case. There does not appear to be any correlation in T_c with the density of states (see Supplemental Material [72]). These results agree with our previous analysis of the susceptibilities: p-wave superconductivity is robust in the ballistic phase but is suppressed in the diffusive phase, while s-wave remains robust well into the localized phase.

Conclusions. Having described the effects of quasiperiodicity on s- and p-wave superconductivity, one might naturally wonder whether these results generalize to other pairing symmetries as well. Owing to a lack of rotation symmetry in the model, there is no sharp distinction between s- and d-wave pairing symmetries. Nevertheless, in the supplement, we present results on spin-singlet nearest neighbor pairing, which reduces to the $d_{x^2-y^2}$ pairing term in the $v \to 0$ limit. We find good qualitative agreement between the p-wave and nearest-neighbor spin-singlet data, suggesting that the essential element resulting in the suppression of the log divergence is not the pairing symmetry, but rather whether the gap integrates to zero over the Brillouin zone.

In summary, we have shown that quasiperiodicity behaves quite unlike random disorder in the context of unconventional superconductivity. We find that p-wave superconductivity is robust up to a finite critical value of the potential strength v_{c1}. This value corresponds to the ballistic-to-diffusive transition of the non-interacting model. s-wave superconductivity, conversely, survives in all three phases: ballistic, diffusive, and localized. Our results do not rule out the possibility of unconventional superconductivity in quasiperiodic twisted trilayer graphene [42]; however, further microscopic studies are necessary to fully explore this possibility.

Acknowledgments. We thank Steve Kivelson, Srinivas Raghu, John Dodaro, Gil Refael, and Rafael Fernandes for insightful discussions. This work was supported in part by a startup fund at Stanford University. E.B. and J.X. were supported by the Israel-USA Binational Science Foundation (BSF) and the European Research Council (ERC) under grant HQMAT (Grant Agreement No. 817799).

[1] A. L. Mackay, Crystallography and the penrose pattern, Physica A **114**, 609 (1982).
[2] L. Bindi, P. J. Steinhardt, N. Yao, and P. J. Lu, Natural quasicrystals, Science **324**, 1306 (2009).
[3] G. Roati, C. D'Errico, L. Fallani, M. Fattori, C. Fort, M. Zaccanti, G. Modugno, M. Modugno, and M. Inguscio, Anderson localization of a non-interacting Bose–Einstein condensate, Nature (London) **453**, 895 (2008).
[4] H. P. Lüschen, S. Scherg, T. Kohlert, M. Schreiber, P. Bordia, X. Li, S. Das Sarma, and I. Bloch, Single-particle mobility edge in a one-dimensional quasiperiodic optical lattice, Phys. Rev. Lett. **120**, 160404 (2018).
[5] D. J. Boers, B. Goedeke, D. Hinrichs, and M. Holthaus, Mobility edges in bichromatic optical lattices, Phys. Rev. A **75**, 063404 (2007).
[6] M. Modugno, Exponential localization in one-dimensional quasi-periodic optical lattices, New J. Phys. **11**, 033023 (2009).
[7] H. Yao, A. Khoudli, L. Bresque, and L. Sanchez-Palencia, Critical behavior and fractality in shallow one-dimensional quasiperiodic potentials, Phys. Rev. Lett. **123**, 070405 (2019).
[8] H. Yao, T. Giamarchi, and L. Sanchez-Palencia, Lieb-liniger bosons in a shallow quasiperiodic potential: Bose glass phase and fractal Mott lobes, Phys. Rev. Lett. **125**, 060401 (2020).
[9] R. Gautier, H. Yao, and L. Sanchez-Palencia, Strongly interacting bosons in a two-dimensional quasicrystal lattice, Phys. Rev. Lett. **126**, 110401 (2021).
[10] Y. Lahini, R. Pugatch, F. Pozzi, M. Sorel, R. Morandotti, N. Davidson, and Y. Silberberg, Observation of a localization transition in quasiperiodic photonic lattices, Phys. Rev. Lett. **103**, 013901 (2009).
[11] P. Wang, Y. Zheng, X. Chen, C. Huang, Y. V. Kartashov, L. Torner, V. V. Konotop, and F. Ye, Localization and delocalization of light in photonic moiré lattices, Nature (London) **577**, 42 (2020).
[12] Y. E. Kraus, Y. Lahini, Z. Ringel, M. Verbin, and O. Zilberberg, Topological states and adiabatic pumping in quasicrystals, Phys. Rev. Lett. **109**, 106402 (2012).
[13] M. Verbin, O. Zilberberg, Y. E. Kraus, Y. Lahini, and Y. Silberberg, Observation of topological phase transitions in photonic quasicrystals, Phys. Rev. Lett. **110**, 076403 (2013).
[14] M. Verbin, O. Zilberberg, Y. Lahini, Y. E. Kraus, and Y. Silberberg, Topological pumping over a photonic Fibonacci quasicrystal, Phys. Rev. B **91**, 064201 (2015).
[15] V. Goblot, A. Štrkalj, N. Pernet, J. L. Lado, C. Dorow, A. Lemaître, L. Le Gratiet, A. Harouri, I. Sagnes, S. Ravets, A. Amo, J. Bloch, and O. Zilberberg, Emergence of criticality through a cascade of delocalization transitions in quasiperiodic chains, Nat. Phys. **16**, 832 (2020).
[16] B. Huang and W. V. Liu, Moiré localization in two-dimensional quasiperiodic systems, Phys. Rev. B **100**, 144202 (2019).
[17] L. Balents, C. R. Dean, D. K. Efetov, and A. F. Young, Superconductivity and strong correlations in moiré flat bands, Nat. Phys. **16**, 725 (2020).
[18] J. F. Karcher, R. Vasseur, and S. Gopalakrishnan, Extended critical phase in quasiperiodic quantum Hall systems, Phys. Rev. B **109**, 064208 (2024)
[19] S. Cheng, R. Asgari, and G. Xianlong, From topological phase to transverse Anderson localization in a two-dimensional quasiperiodic system, Phys. Rev. B **108**, 024204 (2023).
[20] R. Chen, C.-Z. Chen, J.-H. Gao, B. Zhou, and D.-H. Xu, Higher-order topological insulators in quasicrystals, Phys. Rev. Lett. **124**, 036803 (2020).
[21] D. V. Else, S.-J. Huang, A. Prem, and A. Gromov, Quantum many-body topology of quasicrystals, Phys. Rev. X **11**, 041051 (2021).
[22] A. Jagannathan, The Fibonacci quasicrystal: Case study of hidden dimensions and multifractality, Rev. Mod. Phys. **93**, 045001 (2021).
[23] J. H. Pixley, J. H. Wilson, D. A. Huse, and S. Gopalakrishnan, Weyl semimetal to metal phase transitions driven by quasiperiodic potentials, Phys. Rev. Lett. **120**, 207604 (2018).
[24] P. Bordia, H. Lüschen, S. Scherg, S. Gopalakrishnan, M. Knap, U. Schneider, and I. Bloch, Probing slow relaxation and many-body localization in two-dimensional quasiperiodic systems, Phys. Rev. X **7**, 041047 (2017).

[25] T. J. Vongkovit, H. Singh, R. Vasseur, and S. Gopalakrishnan, Effective Luttinger parameter and Kane-Fisher effect in quasiperiodic systems, Phys. Rev. B **110**, L020201 (2024).

[26] T. Cookmeyer, J. Motruk, and J. E. Moore, Critical properties of the ground-state localization-delocalization transition in the many-particle Aubry-André model, Phys. Rev. B **101**, 174203 (2020).

[27] U. Agrawal, S. Gopalakrishnan, and R. Vasseur, Universality and quantum criticality in quasiperiodic spin chains, Nat. Commun. **11**, 2225 (2020).

[28] Y. Yoo, J. Lee, and B. Swingle, Nonequilibrium steady state phases of the interacting Aubry-André-Harper model, Phys. Rev. B **102**, 195142 (2020).

[29] S. Das Sarma and X. C. Xie, Conductance fluctuations in one-dimensional quasicrystals, Phys. Rev. B **37**, 1097 (1988).

[30] D. D. Vu, K. Huang, X. Li, and S. Das Sarma, Fermionic many-body localization for random and quasiperiodic systems in the presence of short- and long-range interactions, Phys. Rev. Lett. **128**, 146601 (2022).

[31] D. D. Vu and S. Das Sarma, Generic mobility edges in several classes of duality-breaking one-dimensional quasiperiodic potentials, Phys. Rev. B **107**, 224206 (2023).

[32] Y.-T. Tu, D. D. Vu, and S. Das Sarma, Avalanche stability transition in interacting quasiperiodic systems, Phys. Rev. B **107**, 014203 (2023).

[33] S.-R. E. Yang and S. Das Sarma, Magnetoexcitons in quasiperiodic superlattices, Phys. Rev. B **37**, 4007 (1988).

[34] M. Gonçalves, J. H. Pixley, B. Amorim, E. V. Castro, and P. Ribeiro, Short-range interactions are irrelevant at the quasiperiodicity-driven Luttinger liquid to Anderson glass transition, Phys. Rev. B **109**, 014211 (2024).

[35] Y. Fu, J. H. Wilson, and J. H. Pixley, Flat topological bands and eigenstate criticality in a quasiperiodic insulator, Phys. Rev. B **104**, L041106 (2021).

[36] Y. Cao, V. Fatemi, S. Fang, K. Watanabe, T. Taniguchi, E. Kaxiras, and P. Jarillo-Herrero, Unconventional superconductivity in magic-angle graphene superlattices, Nature (London) **556**, 43 (2018).

[37] M. Yankowitz, S. Chen, H. Polshyn, Y. Zhang, K. Watanabe, T. Taniguchi, D. Graf, A. F. Young, and C. R. Dean, Tuning superconductivity in twisted bilayer graphene, Science **363**, 1059 (2019).

[38] X. Lu, P. Stepanov, W. Yang, M. Xie, M. A. Aamir, I. Das, C. Urgell, K. Watanabe, T. Taniguchi, G. Zhang, A. Bachtold, A. H. MacDonald, and D. K. Efetov, Superconductors, orbital magnets and correlated states in magic-angle bilayer graphene, Nature (London) **574**, 653 (2019).

[39] G. Chen, A. L. Sharpe, P. Gallagher, I. T. Rosen, E. J. Fox, L. Jiang, B. Lyu, H. Li, K. Watanabe, T. Taniguchi, J. Jung, Z. Shi, D. Goldhaber-Gordon, Y. Zhang, and F. Wang, Signatures of tunable superconductivity in a trilayer graphene moiré superlattice, Nature (London) **572**, 215 (2019).

[40] X. Lai, D. Guerci, G. Li, K. Watanabe, T. Taniguchi, J. Wilson, J. H. Pixley, and E. Y. Andrei, Imaging self-aligned moiré crystals and quasicrystals in magic-angle bilayer graphene on HBN heterostructures, arXiv:2311.07819.

[41] R. Bistritzer and A. H. MacDonald, Moiré bands in twisted double-layer graphene, Proc. Natl. Acad. Sci. USA **108**, 12233 (2011).

[42] A. Uri, S. C. de la Barrera, M. T. Randeria, D. Rodan-Legrain, T. Devakul, P. J. D. Crowley, N. Paul, K. Watanabe, T. Taniguchi, R. Lifshitz, L. Fu, R. C. Ashoori, and P. Jarillo-Herrero, Superconductivity and strong interactions in a tunable moiré quasicrystal, Nature (London) **620**, 762 (2023).

[43] C. Yang, J. May-Mann, Z. Zhu, and T. Devakul, Multi-moiré trilayer graphene: Lattice relaxation, electronic structure, and magic angles, arXiv:2310.12961 [Phys. Rev. B (to be published)].

[44] D. Levine and P. J. Steinhardt, Quasicrystals. I. Definition and structure, Phys. Rev. B **34**, 596 (1986).

[45] D. Levine and P. J. Steinhardt, Quasicrystals: A new class of ordered structures, Phys. Rev. Lett. **53**, 2477 (1984).

[46] F. Setiawan, D.-L. Deng, and J. H. Pixley, Transport properties across the many-body localization transition in quasiperiodic and random systems, Phys. Rev. B **96**, 104205 (2017).

[47] T. Devakul and D. A. Huse, Anderson localization transitions with and without random potentials, Phys. Rev. B **96**, 214201 (2017).

[48] S. Sakai, N. Takemori, A. Koga, and R. Arita, Superconductivity on a quasiperiodic lattice: Extended-to-localized crossover of cooper pairs, Phys. Rev. B **95**, 024509 (2017).

[49] R. N. Araújo and E. C. Andrade, Conventional superconductivity in quasicrystals, Phys. Rev. B **100**, 014510 (2019).

[50] S. Sakai and R. Arita, Exotic pairing state in quasicrystalline superconductors under a magnetic field, Phys. Rev. Res. **1**, 022002(R) (2019).

[51] Y. Cao, Y. Zhang, Y.-B. Liu, C.-C. Liu, W.-Q. Chen, and F. Yang, Kohn-luttinger mechanism driven exotic topological superconductivity on the Penrose lattice, Phys. Rev. Lett. **125**, 017002 (2020).

[52] N. Takemori, R. Arita, and S. Sakai, Physical properties of weak-coupling quasiperiodic superconductors, Phys. Rev. B **102**, 115108 (2020).

[53] R. Ghadimi, T. Sugimoto, K. Tanaka, and T. Tohyama, Topological superconductivity in quasicrystals, Phys. Rev. B **104**, 144511 (2021).

[54] Y. Nagai, Intrinsic vortex pinning in superconducting quasicrystals, Phys. Rev. B **106**, 064506 (2022).

[55] N. Takemori, Superconducting quasicrystals, Isr. J. Chem. **2024**, e202300124 (2024).

[56] Z. Fan, G.-W. Chern, and S.-Z. Lin, Enhanced superconductivity in quasiperiodic crystals, Phys. Rev. Res. **3**, 023195 (2021).

[57] This enhancement near criticality can be understood as a trade-off between maximizing the pairing strength (which is largest when the electrons are locally confined) and global phase coherence (which is low in the localized phase).

[58] P. Anderson, Theory of dirty superconductors, J. Phys. Chem. Solids **11**, 26 (1959).

[59] M. Sigrist and K. Ueda, Phenomenological theory of unconventional superconductivity, Rev. Mod. Phys. **63**, 239 (1991).

[60] A. Keles, A. V. Andreev, B. Z. Spivak, and S. A. Kivelson, Theory of disordered unconventional superconductors, J. Exp. Theor. Phys. **2014**, 1109 (2014).

[61] In principle, however, the phases appearing in the hopping and potential terms can be independent.

[62] Specifically, letting $c \equiv \cos\theta$ and $s \equiv \sin\theta$, we define $\mathbf{R}(\theta) = \begin{pmatrix} c^2+s^3 & cs & cs^2-cs \\ cs & -s & c^2 \\ cs^2-cs & c^2 & c^2s+s^2 \end{pmatrix}$.

[63] K.-H. Bennemann and J. B. Ketterson, *Superconductivity. Volume 1: Conventional and Unconventional Superconductors, Volume 2: Novel Superconductors* (Springer, Berlin, 2008).
[64] J. F. Dodaro and S. A. Kivelson, Generalization of Anderson's theorem for disordered superconductors, Phys. Rev. B **98**, 174503 (2018).
[65] Taking other components of the susceptibility matrix, such as $\chi^0_{\hat{x},\hat{x}}$ or $\chi^0_{\hat{y},\hat{y}}$, has a negligible quantitative and no qualitative effect on the results for the spin-singlet nearest neighbour and p-wave configurations.
[66] Here we keep $\mu/(1+v)$ constant to account for the enlargement of the bandwidth as v increases.
[67] Here $\chi^{\mathrm{s/p}}$ is the susceptibility calculated in the normal state ($\Delta^{\mathrm{s/p}} = 0$).
[68] V. J. Emery and S. A. Kivelson, Importance of phase fluctuations in superconductors with small superfluid density, Nature (London) **374**, 434 (1995).
[69] D. J. Scalapino, S. R. White, and S. Zhang, Insulator, metal, or superconductor: The criteria, Phys. Rev. B **47**, 7995 (1993).
[70] Owing to the anisotropy of the model, the superfluid density need not be the same along every dimension. In practice, however, we find that the densities along each spatial dimension are roughly equal, and therefore appropriately estimated by the geometric mean.
[71] Because Δ varies with position, we take the maximum value of $\Delta_{\boldsymbol{r},\boldsymbol{r}'}$.
[72] See Supplemental Material at http://link.aps.org/supplemental/10.1103/PhysRevB.110.L060501 for details on model characterization and numerics.